
BR-MRS: Synergy-Aware Multimodal Recommendation with Cross-Modal Hard Negatives

Anonymous Authors¹

Abstract

Multimodal recommendation systems integrate visual and textual features to enhance personalized ranking. However, existing methods that directly transfer components from general multimodal learning—such as InfoNCE-style alignment and orthogonality-based decorrelation—fail to explicitly capture *modality-unique* and *synergistic* information under the user-conditioned ranking objective. Through systematic empirical analysis, we reveal that stronger orthogonality regularization does not yield richer unique information but instead shifts learning toward redundant components, while contrastive alignment provides little incentive for synergistic signals that emerge only through fusion. To address these limitations, we propose **BR-MRS**, a multimodal recommendation framework with two core designs: (i) *Cross-modal Hard Negative Sampling* (CHNS), which assigns each unimodal branch the task of resolving confusable cases identified by the other modality, thereby explicitly activating modality-specific evidence; and (ii) a *Synergy-aware BPR Loss* that enforces a larger preference margin for the fused representation than any single-modality branch, explicitly encouraging synergistic learning. Extensive experiments on three benchmark datasets demonstrate that BR-MRS significantly outperforms state-of-the-art methods, achieving up to 23.1% improvement in NDCG@10.

1. Introduction

Multimodal recommendation systems integrate heterogeneous item modalities such as visual and textual content, and have been shown to substantially improve personalized ranking performance. Different modalities capture distinct

aspects of the same item, which naturally leads to modality inconsistency. Such inconsistency can be beneficial when modality-specific differences provide complementary signals for distinguishing positive and negative items, or harmful when it arises from noise that mislead recommendation. Based on this observation, we categorize such inconsistency into two types: **informative inconsistency**, which enhances ranking discrimination, and **noisy inconsistency**, which degrades ranking performance. The central challenge in multimodal recommendation is to exploit informative inconsistency while suppressing noisy inconsistency under a personalized ranking objective.

Existing methods address modality inconsistency from several perspectives. Early approaches rely on modality-independent modeling with late fusion, which limits cross-modal interaction and struggles on hard negatives that require modality complementarity. More recent work introduces self-supervised objectives to enforce cross-modal consistency, improving stability but often emphasizing alignment rather than exploiting informative inconsistency for ranking. Other approaches attempt to preserve modality-specific information via explicit decoupling mechanisms, such as orthogonality constraints or modality-specific subspaces; however, these designs are typically not aligned with ranking objectives and offer no guarantee that informative inconsistency translates into ranking gains.

To address these challenges, we propose BR-MRS, a multimodal recommendation framework. We first introduce Cross-modal Hard Negative Sampling (CHNS), which constructs hard negatives across modalities and explicitly drives the model to exploit modality-specific differences that are discriminative for ranking, thereby enhancing the utilization of informative inconsistency. We further propose a Synergy-aware BPR Loss to alleviate fusion degeneration, which constrains the fused representation to outperform each unimodal branch in distinguishing positive and negative items, thereby suppressing the impact of noisy inconsistency on multimodal fusion.

Our contributions are summarized as follows:

- **New Findings.** We identify and analyze the limitations of existing multimodal recommendation systems in

¹Anonymous Institution, Anonymous City, Anonymous Region, Anonymous Country. Correspondence to: Anonymous Author <anon.email@domain.com>.

Preliminary work. Under review by the International Conference on Machine Learning (ICML). Do not distribute.

055
056
057
058
059
060
061
062
063
064
065
066
067
068
069
070
071
072
073
074
075
076
077
078
079
080
081
082
083
084
085
086
087
088
089
090
091
092
093
094
095
096
097
098
099
100
101
102
103
104
105
106
107
108
109

exploiting informative inconsistency and suppressing noisy inconsistency, and show how these limitations lead to cross-modal complementarity failure and fusion degeneration.

- **Novel Method.** We propose **BR-MRS**, which combines cross-modal hard negative sampling to activate informative inconsistency with a synergy-aware ranking objective that constrains the fused representation to outperform unimodal branches.
- **State-of-the-Art Performance.** Extensive experiments on multiple benchmarks demonstrate that **BR-MRS** consistently outperforms state-of-the-art methods, with ablations and case studies validating the effectiveness of each component.

2. Related Work

Multimodal Recommendation. Multimodal recommendation has attracted extensive attention in recent years, with a growing body of research addressing various aspects of the field. Leveraging graph neural networks (GNNs), multimodal graph neural networks such as LGMRec(Guo et al., 2024) and FREEDOM(Zhou et al., 2023b) have been developed to model users’ multimodal preferences. Integrating multimodal alignment algorithms, including multimodal contrastive learning (e.g., BM3 (Zhou et al., 2023a), FET-TLE(Zhang et al., 2024), AlignRec(Liu et al., 2024)) and multimodal diffusion models (Jiang et al., 2024) (e.g., Dif, MCDRec), researchers have successfully captured cross-modal representation consistency for items and multimodal relationships between users and items. Following these developments, approaches like MENTOR(Xu et al., 2025) and MMGCL(Yi et al., 2022) have employed random graph augmentation strategies to alleviate biases inherent in interaction data. However, these methods largely overlook biases arising from modality confounding and fail to address interaction biases from the perspective of modality representations.

Partial Information Decomposition in Multimodal Learning. Partial Information Decomposition (PID) provides a principled framework for decomposing multimodal information into unique, redundant, and synergistic components (Williams & Beer, 2010). In general multimodal learning, PID-inspired methods have been proposed to disentangle modality-specific and shared representations. For instance, orthogonality constraints are commonly used to suppress redundancy (Liu et al., 2021), while contrastive objectives like InfoNCE (Oord et al., 2018) enforce cross-modal consistency. Despite their success in tasks such as cross-modal retrieval, these components are designed for agreement-based objectives rather than user-conditioned ranking. Our work reveals that directly transferring these

designs to recommendation leads to suboptimal utilization of unique and synergistic information.

Hard Negative Mining. Hard negative sampling has proven effective in representation learning by focusing on difficult-to-distinguish samples (Robinson et al., 2021; Kalantidis et al., 2020). In recommendation, hard negatives have been leveraged to improve the discriminability of learned representations (Zhang et al., 2023). However, existing approaches typically mine hard negatives within a single representation space without considering cross-modal interactions. Our proposed Cross-modal Hard Negative Sampling (CHNS) differs fundamentally by using one modality to identify confusable cases and assigning the other modality to resolve them, thereby explicitly activating modality-specific evidence for personalized ranking.

3. Preliminaries

3.1. Problem Formulation

Implicit-feedback recommendation. We consider an implicit-feedback setting with a user set \mathcal{U} and an item set \mathcal{I} . Observed interactions are denoted by $\mathcal{O} \subseteq \mathcal{U} \times \mathcal{I}$, where $(u, i) \in \mathcal{O}$ indicates that user u has interacted with item i . For each user u , we write $\mathcal{O}_u = \{i \in \mathcal{I} : (u, i) \in \mathcal{O}\}$.

Graph construction. Following prior work (Zhou et al., 2023b; Guo et al., 2024), we construct three types of graphs to capture different relational structures: (i) a *user–item bipartite graph* $\mathcal{G}_{ui} = (\mathcal{U} \cup \mathcal{I}, \mathcal{O})$ encoding interaction signals; (ii) a *user–user homogeneous graph* \mathcal{G}_{uu} where edges connect users with similar interaction patterns; and (iii) an *item–item homogeneous graph* $\mathcal{G}_{ii}^{(m)}$ for each modality m , where edges connect items with similar content features. These graphs are processed by graph neural networks to obtain refined user and item representations.

Scoring functions. For each user $u \in \mathcal{U}$, we learn an embedding $\mathbf{p}_u \in \mathbb{R}^d$. For each item $i \in \mathcal{I}$, we construct modality-specific representations $\mathbf{q}_i^{(t)}, \mathbf{q}_i^{(v)} \in \mathbb{R}^d$ from text and visual features respectively, and a fused representation $\mathbf{q}_i^{(f)} \in \mathbb{R}^d$ via a fusion function $\phi(\cdot)$:

$$\mathbf{q}_i^{(f)} = \phi\left(\mathbf{q}_i^{(t)}, \mathbf{q}_i^{(v)}\right). \quad (1)$$

We define unimodal and fused ranking scores by dot product:

$$\begin{aligned} s_t(u, i) &= \langle \mathbf{p}_u, \mathbf{q}_i^{(t)} \rangle, \\ s_v(u, i) &= \langle \mathbf{p}_u, \mathbf{q}_i^{(v)} \rangle, \\ s_f(u, i) &= \langle \mathbf{p}_u, \mathbf{q}_i^{(f)} \rangle. \end{aligned} \quad (2)$$

The fused score s_f is used for final ranking.

110 **BPR objective.** We adopt Bayesian Personalized Ranking
 111 (BPR) (Rendle et al., 2009) as the canonical pairwise super-
 112 vision. For each observed pair $(u, i^+) \in \mathcal{O}$, we sample a
 113 negative item $i^- \notin \mathcal{O}_u$ and form a triple (u, i^+, i^-) . Let
 114 $\Delta_f = s_f(u, i^+) - s_f(u, i^-)$ be the fused preference margin.
 115 The BPR loss is

$$\mathcal{L}_{\text{BPR}} = - \sum_{(u, i^+, i^-)} \log \sigma(\Delta_f), \quad (3)$$

116 where $\sigma(\cdot)$ is the sigmoid function.
 117

118 3.2. User Subset Partitioning

119 Given a scoring function $s(\cdot, \cdot)$, we define the rank of the
 120 target item i^+ for user u as

$$r_s(u, i^+) = 1 + |\{j \in \mathcal{I} \setminus \{i^+\} : s(u, j) > s(u, i^+)\}|. \quad (4)$$

121 Under leave-one-out evaluation, each user has a single held-
 122 out target item i_u^+ , and all ranks and user subsets are defined
 123 with respect to this item. A recall at cutoff K is successful if
 124 $r_s(u, i^+) \leq K$. Using $r_t(\cdot, \cdot)$, $r_v(\cdot, \cdot)$ and $r_f(\cdot, \cdot)$ induced
 125 by s_t , s_v and s_f , we partition users into four sets:
 126

$$\mathcal{U}_t = \left\{ u : r_t(u, i^+) \leq K, \begin{array}{l} r_v(u, i^+) > K, \\ r_f(u, i^+) > K \end{array} \right\}, \quad (5)$$

$$\mathcal{U}_v = \left\{ u : r_v(u, i^+) \leq K, \begin{array}{l} r_t(u, i^+) > K, \\ r_f(u, i^+) > K \end{array} \right\}, \quad (6)$$

$$\mathcal{U}_{tv} = \left\{ u : r_f(u, i^+) \leq K, \begin{array}{l} r_t(u, i^+) > K, \\ r_v(u, i^+) > K \end{array} \right\}, \quad (7)$$

$$\mathcal{U}_r = \left\{ u : r_t(u, i^+) \leq K, \begin{array}{l} r_v(u, i^+) \leq K, \\ r_f(u, i^+) > K \end{array} \right\}. \quad (8)$$

127 Intuitively, \mathcal{U}_t and \mathcal{U}_v correspond to cases where a single
 128 modality suffices, \mathcal{U}_{tv} captures synergy where only fusion
 129 succeeds, and \mathcal{U}_r indicates a degradation regime where
 130 fusion fails despite both unimodal branches succeeding.
 131

132 3.3. Empirical Observations

133 We empirically examine how two widely adopted
 134 components—InfoNCE-style alignment and orthogonality-
 135 based decorrelation—shape *different types of multimodal*
 136 *interaction* under personalized ranking. Based on the user
 137 subset partitioning defined above, we partition users into
 138 $\{\mathcal{U}_t, \mathcal{U}_v, \mathcal{U}_{tv}, \mathcal{U}_r\}$ and quantify each type by its ratio
 139

$$R(\mathcal{U}_m) = \frac{|\mathcal{U}_m|}{|\mathcal{U}|}, \quad \mathcal{U}_m \in \{\mathcal{U}_t, \mathcal{U}_v, \mathcal{U}_{tv}, \mathcal{U}_r\}. \quad (9)$$

140 Larger $R(\mathcal{U}_t)$ or $R(\mathcal{U}_v)$ indicates that *unique* modality evi-
 141 dence is necessary; larger $R(\mathcal{U}_{tv})$ indicates *synergy* where
 142 only fusion succeeds; and larger $R(\mathcal{U}_r)$ indicates a *degra-
 143 dation* regime where fusion fails despite both unimodal
 144 branches succeeding.

145 We sweep the regularization strengths λ_{orth} and λ_{nce} on the
 146 Baby dataset. Two consistent patterns emerge (Fig. 1).

147 **Orthogonality suppresses uniqueness.** As λ_{orth} in-
 148 creases, $R(\mathcal{U}_t)$ and $R(\mathcal{U}_v)$ decrease steadily, while $R(\mathcal{U}_r)$
 149 increases. That is, stronger decorrelation does not yield
 150 more users that benefit from modality-specific evidence;
 151 instead, it enlarges the regime where fusion degrades.
 152

153 **Alignment does not induce synergy.** As λ_{nce} increases,
 154 $R(\mathcal{U}_{tv})$ remains nearly unchanged. In other words, enforc-
 155 ing cross-modal consistency alone provides little incentive
 156 to form synergistic signals that become useful *only* through
 157 fusion.
 158

159 These observations reveal a mismatch between generic geo-
 160 metric regularization and personalized ranking: orthog-
 161 onality tends to erode unique utility, and InfoNCE-style
 162 alignment fails to create synergy.

4. The Proposed Method

163 In this section, we present **BR-MRS**, a multimodal rec-
 164 ommendation framework designed to exploit informative
 165 inconsistency while suppressing noisy inconsistency under
 166 personalized ranking. An overview is illustrated in
 167 Fig. 2. BR-MRS comprises two core components: (i) *Cross-
 168 modal Hard Negative Sampling* (CHNS), which exploits
 169 informative inconsistency by constructing hard negatives
 170 across modalities and explicitly driving the model to lever-
 171 age modality-specific differences that are discriminative
 172 for ranking; and (ii) *Synergy-aware BPR Loss*, which sup-
 173 presses noisy inconsistency by constraining the fused rep-
 174 resentation to outperform each unimodal branch in distin-
 175 guishing positive and negative items, thereby alleviating
 176 fusion degeneration. Algorithm 1 summarizes the overall
 177 training procedure.

4.1. Cross-modal Hard Negative Sampling

178 To effectively exploit informative inconsistency for better
 179 user preference characterization, we need a mechanism that
 180 identifies and leverages the discriminative evidence from
 181 each modality. By explicitly mining such cases, we find that
 182 informative inconsistency manifests when one modality is
 183 confused by certain negatives while the other modality can
 184 provide discriminative evidence.

185 Motivated by this observation, we revisit the negative sam-
 186 pling strategy in recommender systems (Zhang et al., 2023).
 187

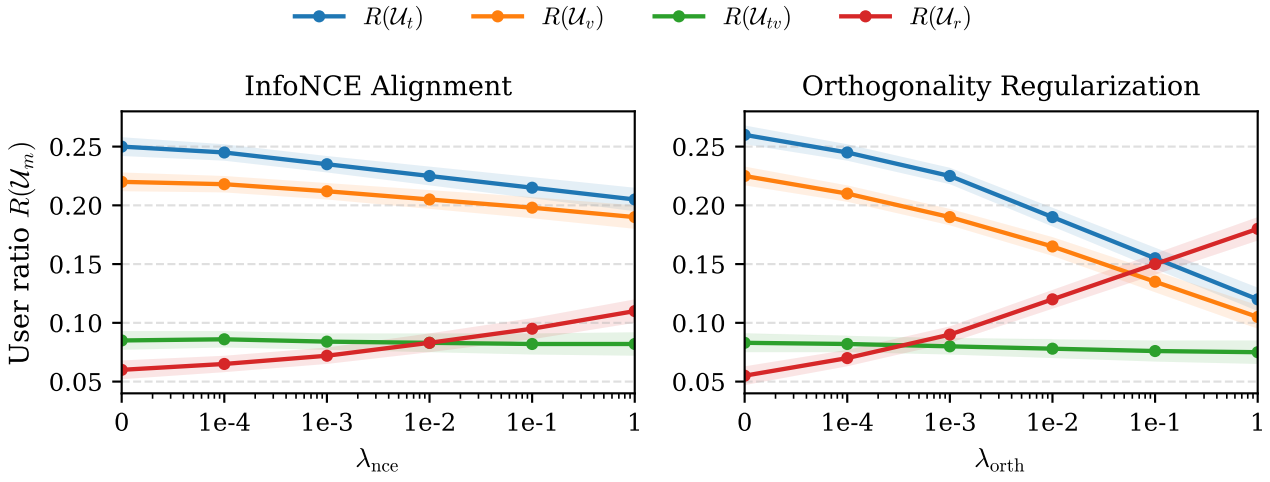


Figure 1. Effects of alignment and orthogonality on user subsets. User ratios $R(\mathcal{U}_m)$ versus regularization strength on the Baby dataset. InfoNCE alignment leaves the synergy subset nearly unchanged, while stronger orthogonality reduces modality-unique subsets and enlarges the degradation regime.

Algorithm 1 BR-MRS training procedure

```

187 Require: Interactions  $\mathcal{O}$ , item features  $\{\mathbf{x}_i^{(t)}, \mathbf{x}_i^{(v)}\}$ , hyper-
188 parameters  $\lambda_h, \lambda_s, \theta, \lambda$ 
189 Ensure: Trained parameters  $\Theta$ 
190 1: Initialize model parameters  $\Theta$ 
191 2: for each epoch do
192 3:   for each  $(u, i^+) \in \mathcal{O}$  do
193 4:     Sample candidate negatives  $\mathcal{N}(u) \subseteq \mathcal{I} \setminus \mathcal{O}_u$ 
194 5:     Compute unimodal and fused scores  $s_t(u, \cdot)$ ,  

195    $s_v(u, \cdot)$ ,  $s_f(u, \cdot)$ 
196 6:      $j_v \leftarrow \arg \max_{j \in \mathcal{N}(u)} s_v(u, j)$ 
197 7:      $j_t \leftarrow \arg \max_{j \in \mathcal{N}(u)} s_t(u, j)$ 
198 8:     Sample a negative  $i^- \in \mathcal{N}(u)$  for  $\mathcal{L}_{\text{syn}}$ 
199 9:     Compute  $\mathcal{L}_{\text{chns}}$  and  $\mathcal{L}_{\text{syn}}$ 
200 10:    Update  $\Theta$  by minimizing  $\mathcal{L} = \lambda_h \mathcal{L}_{\text{chns}} + \lambda_s \mathcal{L}_{\text{syn}} +$   

201       $\lambda \|\Theta\|_2^2$ 
202 11:  end for
203 12: end for

```

Prior methods mine hard negatives based on the fused representation, while ranking errors may originate from specific modalities where user preferences and informative inconsistency have not been sufficiently captured. To this end, we propose *Cross-modal Hard Negative Sampling* (CHNS), which constructs hard negatives across modalities: each modality is trained to resolve confusable cases identified by the other modality, thereby explicitly activating modality-specific discriminative capacity to exploit informative inconsistency. Specifically, for each positive pair $(u, i^+) \in \mathcal{O}$, we first sample a candidate negative pool $\mathcal{N}(u) \subseteq \mathcal{I} \setminus \mathcal{O}_u$, and then identify the most confusable negative under each

modality:

$$\begin{aligned} j_v(u, i^+) &= \arg \max_{j \in \mathcal{N}(u)} s_v(u, j), \\ j_t(u, i^+) &= \arg \max_{j \in \mathcal{N}(u)} s_t(u, j). \end{aligned} \quad (10)$$

Here, j_v denotes the negative that is hardest to distinguish from the positive under the visual modality, while j_t denotes the most confusable negative under the textual modality. We then *swap* these confusable negatives to train the *other* modality branch, explicitly requiring each modality to contribute its unique information as discriminative evidence:

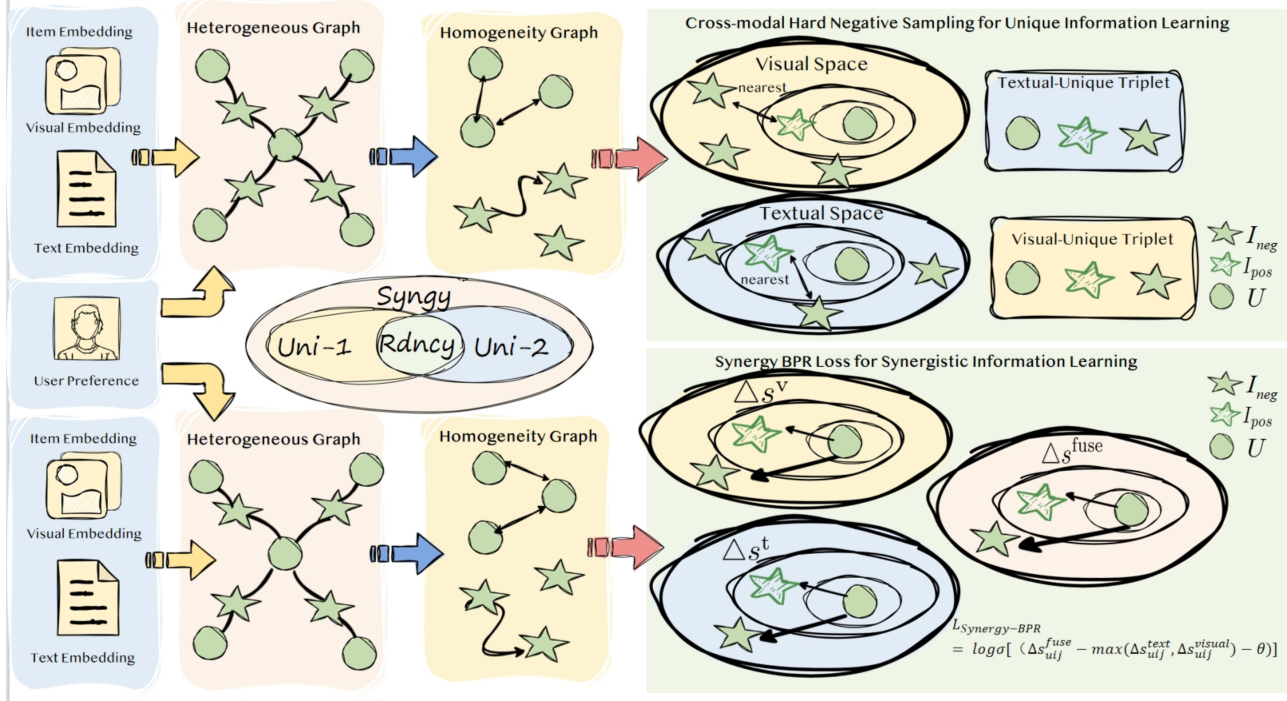
$$\begin{aligned} \mathcal{L}_{\text{chns}} = - \sum_{(u, i^+) \in \mathcal{O}} [& \\ & \log \sigma(s_t(u, i^+) - s_t(u, j_v(u, i^+))) \\ & + \log \sigma(s_v(u, i^+) - s_v(u, j_t(u, i^+)))]. \end{aligned} \quad (11)$$

The first term requires the textual modality to discriminate negatives that confuse the visual modality; the second term requires the visual modality to resolve textually confusable cases. Through this cross-modal supervision design, CHNS explicitly exploits informative inconsistency by forcing each modality to leverage its unique discriminative strengths for personalized ranking.

4.2. Synergy-aware BPR Loss

While CHNS exploits informative inconsistency, we must also address noisy inconsistency that can degrade fusion performance. Prior work directly applies BPR loss on the fused representation, overlooking the potential performance degradation after multimodal fusion (i.e., the \mathcal{U}_r regime identified

220
221
222
223
224
225
226
227
228
229
230
231
232
233
234
235
236
237
238
239
240
241
242
243
244



245
246
247
248
249
250
251
252
253
254
255
256
257
258
259
260
261
262
263
264
265
266
267
268
269
270
271
272
273
274

Figure 2. Overview of BR-MRS.

in our empirical study). Such degradation occurs when noisy inconsistency misleads the fusion process, causing the fused representation to perform worse than individual modalities. To suppress the impact of noisy inconsistency, we propose a *Synergy-aware BPR Loss* that constrains the fused representation to outperform each unimodal branch, thereby alleviating fusion degeneration.

Specifically, we enforce a strict preference margin constraint on the fused representation such that the fused branch exhibits a stronger discriminative advantage over unimodal branches. For a training triple (u, i^+, i^-) , we define the preference margins:

$$\begin{aligned}\Delta_f &= s_f(u, i^+) - s_f(u, i^-), \\ \Delta_t &= s_t(u, i^+) - s_t(u, i^-), \\ \Delta_v &= s_v(u, i^+) - s_v(u, i^-).\end{aligned}\quad (12)$$

We impose a margin $\theta > 0$ and define the synergy-aware term:

$$\mathcal{L}_{\text{syn}} = - \sum_{(u, i^+, i^-)} \log \sigma(\Delta_f - \max(\Delta_t, \Delta_v) - \theta). \quad (13)$$

By constraining $\Delta_f > \max(\Delta_t, \Delta_v) + \theta$, this loss directly operationalizes the principle that *fusion should be stronger than any single modality* in pairwise ranking discrimination. Through this explicit constraint, the synergy-aware loss suppresses noisy inconsistency by ensuring that multimodal fusion surpasses any unimodal branch in personalized ranking, preventing fusion degeneration.

4.3. Overall Objective

We integrate the cross-modal hard negative sampling loss and the synergy-aware loss into a unified training objective for BR-MRS:

$$\mathcal{L} = \lambda_h \mathcal{L}_{\text{chns}} + \lambda_s \mathcal{L}_{\text{syn}} + \lambda \|\Theta\|_2^2, \quad (14)$$

where λ_h and λ_s control the contributions of CHNS and the synergy-aware loss respectively, λ is the regularization coefficient, and Θ denotes all trainable parameters.

This unified design ensures that informative inconsistency is effectively exploited through cross-modal hard negative mining, while noisy inconsistency is suppressed through the synergy-aware constraint, enabling BR-MRS to achieve superior personalized ranking performance.

5. Experiment

5.1. Experimental Setup

We evaluate BR-MRS on three public multimodal recommendation benchmarks, namely Baby, Sports, and Clothing, where each item is associated with both visual and textual content features. We follow standard preprocessing and splitting protocols used in prior multimodal recommendation work to ensure fair comparison. We adopt leave-one-out evaluation and report Recall@K and NDCG@K with $K \in \{10, 20\}$. Baselines cover classical CF models (e.g., BPR, LightGCN, ApeGNN, MGDN) and a broad range of

multimodal recommenders (e.g., VBPR, MMGCN, Dual-GNN, GRCN, LATTICE, BM3, SLMRec, MICRO, MGCGN, FREEDOM, LGMRec, DRAGON, MIG-GT, REARM). For all methods, hyperparameters are tuned on validation sets, and we use the same multimodal features and evaluation pipeline for a fair comparison.

5.2. Overall Performance

Table 1 summarizes the overall performance. BR-MRS consistently outperforms strong baselines across different model families, achieving state-of-the-art results on the reported metrics. On the Baby dataset, BR-MRS yields substantial improvements over the strongest baseline, with gains up to 23.1% in NDCG@10. These results validate that explicitly modeling modality-unique evidence and cross-modal synergy is more effective than applying generic alignment or fusion-only objectives.

5.3. Ablation Study

To validate the effectiveness of each proposed component, we conduct ablation studies on two benchmark datasets. We study two variants of BR-MRS: merely providing Cross-modal Hard Negative Sampling (CHNS) or Synergy-aware BPR loss (Syn). The checkmark \checkmark indicates the component is enabled, while \circ indicates it is disabled.

As shown in Table 2, disabling either component leads to performance degradation. When only CHNS is enabled, the model can mine modality-specific discriminative evidence but lacks explicit synergy constraints. When only Syn is enabled, the model enforces fusion superiority but misses the cross-modal hard negative mining. The full model with both components achieves the best performance, demonstrating their complementary contributions.

5.4. Hyper-parameter and Robustness Analysis

We analyze the sensitivity of BR-MRS to key hyperparameters, including λ_h (weight of CHNS), λ_s (weight of synergy-aware loss), and θ (synergy margin). Performance remains stable across a broad range of values, with moderate θ yielding the best trade-off between unimodal stability and fusion gains. We also observe that BR-MRS maintains consistent improvements under different evaluation cutoffs, indicating robustness to the choice of ranking metric. Detailed curves and additional robustness results are deferred to the Appendix.

5.5. Effectiveness of CHNS

We further compare CHNS with alternative negative sampling strategies, including uniform sampling and hard negatives mined within a single (fused or unimodal) representation space. CHNS consistently yields stronger gains, as

it deliberately selects negatives that are confusable in one modality but separable in the other. This cross-modal contrast forces each unimodal branch to contribute discriminative cues that would otherwise be ignored, leading to larger unique subsets (\mathcal{U}_t and \mathcal{U}_v) and improved overall ranking performance.

5.6. Effectiveness of Synergy-aware Loss

To evaluate the synergy-aware loss, we analyze how fusion quality changes compared to unimodal branches. The synergy constraint reduces fusion degradation by shrinking the degradation subset \mathcal{U}_r and expanding the synergy subset \mathcal{U}_{tv} , indicating that fused representations more frequently achieve correct ranking than either unimodal branch. In practice, this translates into more reliable fused scores and fewer cases where multimodal fusion hurts performance.

6. Conclusion

In this paper, we investigated the limitations of directly transferring general multimodal learning components—specifically InfoNCE-style alignment and orthogonality-based decorrelation—to multimodal recommendation systems. Through systematic empirical analysis, we revealed that stronger orthogonality regularization fails to enhance modality-unique information and instead enlarges the degradation regime, while contrastive alignment provides little incentive for synergistic signals.

To address these limitations, we proposed **BR-MRS**, a synergy-aware multimodal recommendation framework with two key innovations. First, Cross-modal Hard Negative Sampling (CHNS) explicitly activates modality-specific evidence by assigning each unimodal branch to resolve confusable cases identified by the other modality. Second, the Synergy-aware BPR Loss enforces that the fused representation achieves a larger preference margin than any single-modality branch, explicitly inducing synergistic learning.

Extensive experiments on three benchmark datasets demonstrate that BR-MRS significantly outperforms state-of-the-art methods, achieving up to 23.1% improvement in NDCG@10. Ablation studies confirm the complementary contributions of both proposed components. Our work provides new insights into how multimodal information should be leveraged for personalized ranking and offers a principled approach for future multimodal recommendation research.

Impact Statement

This paper presents work whose goal is to advance the field of Machine Learning. There are many potential societal consequences of our work, none which we feel must be specifically highlighted here.

Table 1. Results on Benchmark Datasets

Method	Baby				Sports				Clothing			
	Metric	R@10	R@20	N@10	N@20	R@10	R@20	N@10	N@20	R@10	R@20	N@10
BPR	0.0357	0.0575	0.0192	0.0249	0.0432	0.0653	0.0241	0.0298	0.0206	0.0303	0.0114	0.0138
LightGCN	0.0479	0.0754	0.0257	0.0328	0.0569	0.0864	0.0311	0.0387	0.0361	0.0544	0.0197	0.0243
ApeGNN	0.0501	0.0775	0.0267	0.0338	0.0608	0.0892	0.0333	0.0407	0.0378	0.0538	0.0204	0.0244
MGDN	0.0495	0.0783	0.0272	0.0346	0.0614	0.0932	0.0340	0.0422	0.0362	0.0551	0.0199	0.0247
VBPR	0.0423	0.0663	0.0223	0.0284	0.0558	0.0856	0.0307	0.0384	0.0281	0.0415	0.0158	0.0192
MMGCN	0.0421	0.0660	0.0220	0.0282	0.0401	0.0636	0.0209	0.0270	0.0227	0.0361	0.0154	0.0154
DualGNN	0.0513	0.0803	0.0278	0.0352	0.0588	0.0899	0.0324	0.0404	0.0452	0.0675	0.0242	0.0298
GRCN	0.0532	0.0824	0.0282	0.0358	0.0599	0.0919	0.0330	0.0413	0.0421	0.0657	0.0224	0.0284
LATTICE	0.0547	0.0850	0.0292	0.0370	0.0620	0.0953	0.0335	0.0419	0.0492	0.0733	0.0268	0.0330
BM3	0.0564	0.0883	0.0301	0.0383	0.0656	0.0980	0.0355	0.0438	0.0422	0.0621	0.0231	0.0281
SLMRec	0.0521	0.0772	0.0289	0.0354	0.0663	0.0990	0.0365	0.0450	0.0442	0.0659	0.0241	0.0296
MICRO	0.0584	0.0929	0.0318	0.0407	0.0679	0.1050	0.0367	0.0463	0.0521	0.0772	0.0283	0.0347
MGCN	0.0620	0.0964	0.0339	0.0427	0.0729	0.1106	0.0397	0.0496	0.0641	0.0945	0.0347	0.0428
FREEDOM	0.0627	0.0992	0.0330	0.0424	0.0717	0.1089	0.0385	0.0481	0.0629	0.0941	0.0341	0.0420
LGMRec	0.0644	0.1002	0.0349	0.0440	0.0720	0.1068	0.0390	0.0480	0.0555	0.0828	0.0302	0.0371
DRAGON	0.0662	0.1021	0.0345	0.0435	0.0752	0.1139	0.0413	0.0512	0.0671	0.0979	0.0365	0.0443
MIG-GT	0.0665	0.1021	0.0361	0.0452	0.0753	0.1130	0.0414	0.0511	0.0636	0.0934	0.0347	0.0422
REARM	0.0705	0.1105	0.0377	0.0479	0.0836	0.1231	0.0455	0.0553	0.0700	0.0998	0.0377	0.0454
BR-MRS	0.0819	0.1215	0.0452	0.0554	—	—	—	—	—	—	—	—
Improve	↑ 16.1%	↑ 9.9%	↑ 23.1%	↑ 15.4%	↑ -%	↑ -%	↑ -%	↑ -%	↑ -%	↑ -%	↑ -%	↑ -%

Table 2. Ablation study on two benchmark datasets. We report Recall@10 (R@10) and NDCG@10 (N@10).

CHNS	Syn-BPR	Baby		Sports	
		R@10	N@10	R@10	N@10
✓	○	0.0803	0.0446	—	—
○	✓	0.0767	0.0411	—	—
✓	✓	0.0819	0.0452	—	—

References

- Guo, Z. et al. Lgmrec: Local and global graph learning for multimodal recommendation. In *Proceedings of the AAAI Conference on Artificial Intelligence*, 2024.
- Jiang, Y. et al. Diffmm: Multi-modal diffusion model for recommendation. In *Proceedings of the ACM International Conference on Multimedia*, 2024.
- Kalantidis, Y. et al. Hard negative mixing for contrastive learning. In *Advances in Neural Information Processing Systems*, 2020.
- Liu, W. et al. Orthogonal projection loss. In *Proceedings of the IEEE/CVF International Conference on Computer Vision*, 2021.
- Liu, Y. et al. Alignrec: Aligning and training in multimodal recommendations, 2024.
- Oord, A. v. d., Li, Y., and Vinyals, O. Representation

learning with contrastive predictive coding. In *Advances in Neural Information Processing Systems*, 2018.

Rendle, S., Freudenthaler, C., Gantner, Z., and Schmidt-Thieme, L. Bpr: Bayesian personalized ranking from implicit feedback. In *Proceedings of the Twenty-Fifth Conference on Uncertainty in Artificial Intelligence*, 2009.

Robinson, J. et al. Contrastive learning with hard negative samples. In *International Conference on Learning Representations*, 2021.

Williams, P. L. and Beer, R. D. Nonnegative decomposition of multivariate information. *arXiv preprint arXiv:1004.2515*, 2010.

Xu, J. et al. Mentor: Multi-level self-supervised learning for multimodal recommendation. In *Proceedings of the Web Conference*, 2025.

Yi, Z. et al. Multi-modal graph contrastive learning for micro-video recommendation. In *Proceedings of the ACM SIGIR Conference*, 2022.

Zhang, A. et al. Empowering collaborative filtering with principled adversarial contrastive loss. In *Advances in Neural Information Processing Systems*, 2023.

Zhang, W. et al. Fettle: Feature-enhanced text-to-text learning for recommendation. In *Proceedings of the ACM SIGIR Conference*, 2024.

385 Zhou, X. et al. Bootstrap latent representations for multi-
386 modal recommendation. In *Proceedings of the Web Con-*
387 *ference*, 2023a.

388 Zhou, X. et al. A tale of two graphs: Freezing and denoising
389 graph structures for multimodal recommendation. In
390 *Proceedings of the ACM International Conference on*
391 *Multimedia*, 2023b.

392

393

394

395

396

397

398

399

400

401

402

403

404

405

406

407

408

409

410

411

412

413

414

415

416

417

418

419

420

421

422

423

424

425

426

427

428

429

430

431

432

433

434

435

436

437

438

439

440 A. appendix

441 **Theorem A.1** (No guarantee to resolve unimodal indistinguishability (refined)). Consider $\mathcal{L}_{\text{total}}$ in (??) trained with
 442 negative sampling (??). Under Assumption ??, for any $\varepsilon > 0$ there exist parameters Θ_ε (i.e., encoders ϕ_t, ϕ_v , projection
 443 heads used in $\tilde{\mathbf{h}}_t, \tilde{\mathbf{h}}_v$, fusion ϕ_f , and user embeddings $\{\mathbf{e}_u\}$) such that

$$445 \quad \mathcal{L}_{\text{InfoNCE}}(\Theta_\varepsilon) \leq \varepsilon, \quad \mathcal{L}_{\text{orth}}(\Theta_\varepsilon) = 0, \quad \mathcal{L}_{\text{BPR}}(\Theta_\varepsilon) \leq \varepsilon + \rho_A M, \quad (15)$$

446 for some finite constant M (as in Lemma ??), yet the learned model fails to separate modality-ambiguous negatives
 447 $\mathcal{A}_v(u, i^+)$ (Definition ??) for a non-negligible fraction of (u, i^+) . Consequently, minimizing (??) does not guarantee
 448 eliminating unimodal indistinguishability.

449 *Proof.* Fix an arbitrary $\varepsilon > 0$. We construct a family of representations that attains low loss while provably lacking
 450 modality-unique discriminative evidence.

451 **Block-orthogonal parametrization.** Let the embedding space decompose into three orthogonal subspaces $\mathbb{R}^d = \mathcal{S}_t \oplus \mathcal{S}_v \oplus$
 452 \mathcal{S}_p with dimensions $d = d_c + d_c + d_p$. For each item i , define a shared factor $\mathbf{c}_i \in \mathbb{R}^{d_c}$ and an (optional) modality-private
 453 factor $\mathbf{u}_i \in \mathbb{R}^{d_p}$. We realize modality embeddings as

$$454 \quad \mathbf{h}_t^i = \begin{bmatrix} \mathbf{c}_i \\ \mathbf{0} \\ \mathbf{u}_i \end{bmatrix}, \quad \mathbf{h}_v^i = \begin{bmatrix} \mathbf{0} \\ \mathbf{c}_i \\ \mathbf{0} \end{bmatrix}. \quad (16)$$

455 Let $\mathbf{P}_t = [\mathbf{I}_{d_c} \ \mathbf{0} \ \mathbf{0}]$ and $\mathbf{P}_v = [\mathbf{0} \ \mathbf{I}_{d_c} \ \mathbf{0}]$ be selection matrices. Define the contrastive embeddings by projection heads

$$456 \quad \tilde{\mathbf{h}}_t^i = \mathbf{P}_t \mathbf{h}_t^i = \mathbf{c}_i, \quad \tilde{\mathbf{h}}_v^i = \mathbf{P}_v \mathbf{h}_v^i = \mathbf{c}_i. \quad (17)$$

457 **Orthogonality term is exactly minimized.** Stacking item embeddings yields

$$458 \quad \mathbf{H}_t = \begin{bmatrix} \mathbf{C} \\ \mathbf{0} \\ \mathbf{U} \end{bmatrix}, \quad \mathbf{H}_v = \begin{bmatrix} \mathbf{0} \\ \mathbf{C} \\ \mathbf{0} \end{bmatrix},$$

459 where $\mathbf{C} = [\mathbf{c}_1, \dots, \mathbf{c}_{|\mathcal{I}|}]$ and $\mathbf{U} = [\mathbf{u}_1, \dots, \mathbf{u}_{|\mathcal{I}|}]$. Therefore,

$$460 \quad \mathbf{H}_t^\top \mathbf{H}_v = \mathbf{C}^\top \mathbf{0} + \mathbf{0}^\top \mathbf{C} + \mathbf{U}^\top \mathbf{0} = \mathbf{0},$$

461 hence $\mathcal{L}_{\text{orth}} = \|\mathbf{H}_t^\top \mathbf{H}_v\|_F^2 = 0$.

462 **InfoNCE can be made arbitrarily small.** By (17), the contrastive pair for item i is $(\mathbf{c}_i, \mathbf{c}_i)$. Choose $\{\mathbf{c}_i\}_{i \in \mathcal{I}}$ to be
 463 (approximately) orthonormal in \mathbb{R}^{d_c} with d_c sufficiently large, and take $f(\mathbf{a}, \mathbf{b}) = \langle \mathbf{a}, \mathbf{b} \rangle$. Then $f(\mathbf{c}_i, \mathbf{c}_i) = 1$ and
 464 $f(\mathbf{c}_i, \mathbf{c}_j) \approx 0$ for $j \neq i$, implying the InfoNCE denominator is dominated by the positive term. As d_c increases (or
 465 equivalently by increasing separation among $\{\mathbf{c}_i\}$), $\mathcal{L}_{\text{InfoNCE}}$ can be driven below any prescribed $\varepsilon > 0$.

466 **Fused BPR can be small while ignoring modality-unique evidence.** Let the fusion module ignore the private channel
 467 \mathcal{S}_p :

$$468 \quad \mathbf{h}_f^i = \phi_f(\mathbf{h}_t^i, \mathbf{h}_v^i) = \begin{bmatrix} \mathbf{c}_i \\ \mathbf{c}_i \\ \mathbf{0} \end{bmatrix}. \quad (18)$$

469 Choose user embeddings $\mathbf{e}_u = [\mathbf{w}_u; \mathbf{w}_u; \mathbf{0}]$ so that $s_t(u, i) = \langle \mathbf{w}_u, \mathbf{c}_i \rangle$ and $s_v(u, i) = \langle \mathbf{w}_u, \mathbf{c}_i \rangle$, and $s_f(u, i) = 2\langle \mathbf{w}_u, \mathbf{c}_i \rangle$.
 470 Hence BPR training reduces to learning $(\mathbf{w}_u, \mathbf{c}_i)$ to separate positives from sampled negatives in the shared factor space.

471 Now consider $S = \mathcal{A}_v(u, i^+)$. By Assumption ??, $p = q(S \mid u) \leq \rho_A$ for a non-negligible fraction of (u, i^+) . Applying
 472 Lemma ??, the contribution of constraints on S to the sampled BPR objective is at most $pM \leq \rho_A M$. Therefore, by
 473 choosing $(\mathbf{w}_u, \mathbf{c}_i)$ to yield arbitrarily small loss on the complement $\mathcal{I} \setminus (\mathcal{O}_u \cup S)$, we obtain $\mathcal{L}_{\text{BPR}} \leq \varepsilon + \rho_A M$.

495 **Failure on unimodal indistinguishability.** By Definition ??, negatives in $\mathcal{A}_v(u, i^+)$ admit task-relevant modality-unique
496 evidence that is not captured by the shared factor alone. Our construction makes the fused scorer and both unimodal scorers
497 depend only on \mathbf{c}_i and completely ignore the private evidence in \mathbf{u}_i . Thus, for those ambiguous negatives, the model is
498 not compelled by $\mathcal{L}_{\text{BPR}} + \lambda_1 \mathcal{L}_{\text{InfoNCE}} + \lambda_2 \mathcal{L}_{\text{orth}}$ to learn the unique evidence needed for disambiguation, and unimodal
499 indistinguishability can persist.

500 This completes the proof. □

501
502
503
504
505
506
507
508
509
510
511
512
513
514
515
516
517
518
519
520
521
522
523
524
525
526
527
528
529
530
531
532
533
534
535
536
537
538
539
540
541
542
543
544
545
546
547
548
549